Imaging patterns of intensity in topographically directed photolithography

Kateri E. Paul, Tricia L. Breen, Tanja Hadzik, and George M. Whitesides[a)]
Department of Chemistry and Chemical Biology, Harvard University, 12 Oxford Street, Cambridge, Massachusetts 02138

Stephen P. Smith and Mara Prentiss
Department of Physics, Harvard University, Cambridge, Massachusetts 02138

This article describes a process that consists of embossing a bas-relief pattern into the surface of a layer of photoresist and flood illuminating the embossed resist; this process uses the topography of the resist to generate a pattern of optical intensity inside the resist layer. Development of embossed, illuminated ($\lambda = 365-436$ nm) photoresist yields structures as small as 70 nm. Numerical solutions of the Fresnel integral are used to calculate the pattern of intensity of light in the photoresist layer. Numeric simulation of a nondiffusion-limited development process results in theoretical structures that correlate well with the structures generated experimentally. © *2005 American Vacuum Society.* [DOI: 10.1116/1.1924415]

I. INTRODUCTION

Conventional photolithography typically projects an image patterned in an opaque layer of chromium on a rigid quartz mask onto a layer of photoresist;[1,2] a typical optical reduction factor is 5×. Improvements applied to this technique to decrease the feature sizes it generates include using short wavelengths of light, phase-shifting masks, off-axis illumination, and optical proximity correction.[3] These adjustments may cause other difficulties, however. Using wavelengths of light <250 nm necessitates changes to exposure tools and resist systems; photolithographic masks are rigid, fragile, expensive, difficult to repair, and their characteristics limit them to two dimensional (2D) patterning of flat surfaces. Most of the techniques for generating arrays of nanoscopic features are available only to a few researchers with access to specialized and expensive facilities. We wish to develop techniques for nanofabrication that are accessible to a wide range of researchers, and are more flexible in the geometries and chemical entities they can pattern than those now available.

Topographically directed photolithography (TOP),[4] like other soft lithographic techniques,[5,6] uses an elastomeric mold patterned with micron-sized features as a pattern-transfer element. In this technique, the elastomeric mold is used to emboss a pattern on a layer of photoresist;[7] the topography on the surface of the resist layer is then used to pattern flood illumination into selected regions of the resist layer. After development of exposed photoresist, TOP generates 70–200 nm features. TOP uses elastomeric molds patterned on masters that are commercially available or generated by photolithography and soft lithography. Thin molds can conform to both flat and cylindrically or spherically curved surfaces.[8,9] The technique is simple, easy to use, inexpensive, and available to a large number of researchers. It is, however, more restricted in its applications than

projection photolithography. Nonetheless, for certain applications—optical devices, patterning of curved or spherical surfaces, and rapidly generating 100 nm scale masters when lateral pattern fidelity is not critically important—it is superior.

This article demonstrates that structures generated by TOP agree with theoretical predictions. We examine the 2D patterns generated after exposure and development of thick layers of photoresist whose surface was patterned with topographical relief. We compare these structures to theoretical structures generated using the Fresnel–Kirchoff theory to calculate the 2D pattern of intensity in the photoresist, followed by a numerical simulation of the development of the photoresist. We begin with a qualitative description of the experimental technique, and follow with a description of the generation of theoretical intensity patterns. We then describe and analyze the structures generated in photoresist, and compare these structures with those predicted theoretically.

II. EXPERIMENT

We prepared poly(dimethylsiloxane) (PDMS), (Sylgard 184, Dow Corning, Midland, MI) using a ratio of 6:1 prepolymer to curing agent.[10] This ratio provides PDMS molds that are stiffer than the recommended 10:1 ratio; it also minimizes sagging of features. After degassing the mixture under vacuum, we poured the PDMS liquid prepolymer over the master and cured it in an oven at 65 °C for at least 2 h. Masters were prepared using several techniques: conventional photolithography was used for rectangular gratings; soft lithography for microlenses;[11] and commercially available masters, such as holographic diffraction gratings (Edmund Scientific, Barrington, N.J.), for sinusoidal surface structures. For masters produced using conventional photolithography, we controlled the thickness of the photoresist layer by tuning the speed used in spin casting the resist, and therefore the height of the features. Amplitude masks were chromium on soda-lime glass and were obtained from Advanced Reproductions (North Andover, Mass.)[12] or Photron-

---

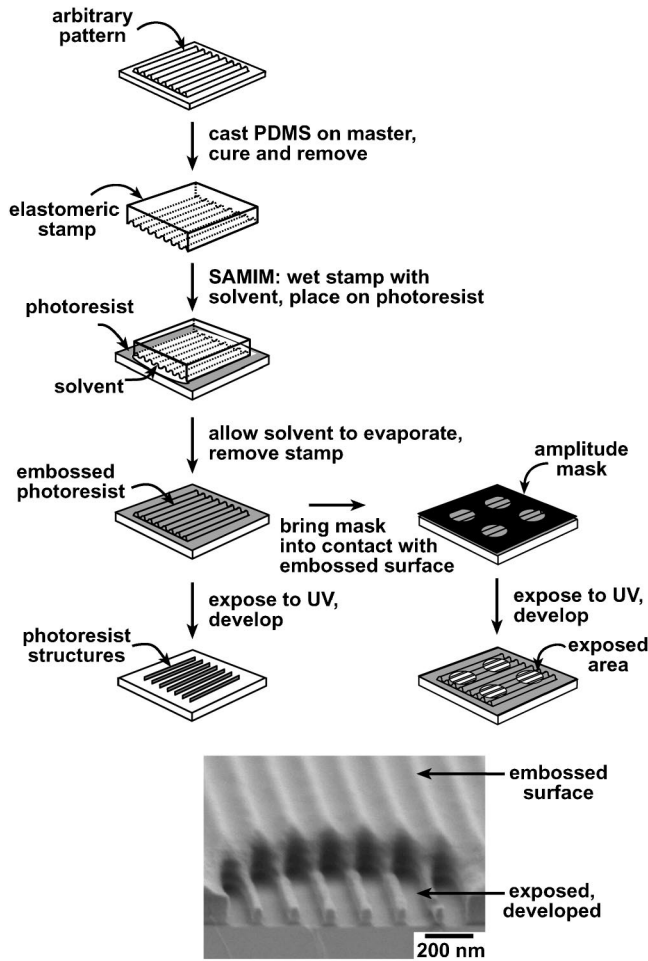[a)]Electronic mail: gwhitesides@gmwgroup.harvard.edu

FIG. 1. Schematic showing the procedure used to form photoresist features using TOP. Casting prepolymer against commercially available masters or those generated by conventional photolithography or soft lithography generates PDMS molds. A small amount of solvent is applied to the surface of the PDMS mold and the mold is placed in contact with a layer of photoresist spin coated on a silicon wafer. When the solvent dissipates, the mold is removed revealing its pattern in bas relief on the photoresist layer. The photoresist is then either exposed directly to flood-UV light or exposed through an amplitude mask and developed. For simplicity, the schematic and SEM image at the bottom show patterns generated on a thin layer of resist.

ics (Brookfield, Ct).[13] Profilometry (Tencor Alpha Step 200) determined the thickness of the photoresist layer on the masters.

Figure 1 shows the procedure used in TOP. Molds of PDMS were removed from the masters and used with solvent-assisted embossing as described previously[4,7] to generate topography on the surface of the photoresist layer. A small amount of 2-propanol was applied to the surface of the PDMS mold using a cleanroom-compatible cloth, and the mold was placed in contact with a layer of photoresist. Photoresist layers were spun on $\langle 100 \rangle$ silicon wafers (Silicon Sense, Nashua, N.H.). We used a photoresist layer with thickness greater than 4 μm (Shipley STR 1045, Marlboro, Mass.) to ensure that the intensity pattern was recorded solely in the photoresist and did not reach (or reflect from) the silicon substrate. Rogers and co-workers have shown another benefit to using thick polymer layers: they can also

yield a complex 3D polymer nanostructure when crosslinked by illumination through PDMS near-field phase shifting mask, followed by careful development.[14]

The solvent formed a liquid-like gel with the photoresist that flowed into the features on the surface of the mold. When the solvent had dissipated through the resist layer and the PDMS mold ($\sim$5–10 min) the mold was removed; the topography of the mold was embossed in bas–relief in the surface of the photoresist layer. The embossed photoresist was either exposed through an amplitude mask or directly to flood-ultraviolet (UV) light (365–436 nm) using a Karl Süss (MJB3 400) mask aligner, developed for 1 min in Shipley Micoposit 452, and rinsed in 18 MΩ water. Samples were examined using a LEO 982 digital scanning electron microscope. We cleaved the silicon substrate perpendicular to lines embossed on the surface of the photoresist, mounted the cleaved edge on a block, and examined the profile of the exposed photoresist surface at 15° from normal. We used accelerating voltages at or below 1 keV to minimize charging of the photoresist.

III. RESULTS AND DISCUSSION

A. Choice of photosensitive polymer system

Many positive and so-called image-reversal resists are two-component systems that consist of a cresol Novolak resin and a diazonapthoquinone compound; the latter acts as the photosensitizer. The photosensitizer in these resists releases N_2 when activated by incident light and generates a carboxylic acid group that renders the exposed area soluble in a basic developing solution to give a positive resist image. Image reversal resists can operate in either conventional (positive mode), or image-reversal (negative mode). To reverse the positive image to negative tone, the exposed photoresist layer is subjected to a postexposure bake causing the exposed area to crosslink via an acid-catalyzed reaction. Crosslinking renders the area impervious to further exposure and insoluble in developer. The areas of photoresist protected by a mask in the first exposure are then made soluble by a second, flood exposure of the resist layer.

Previous research in this group studying the intensity patterns of light transferred into a photoresist layer through a PDMS phase mask used AZ 5200 series resist in image-reversal mode as the medium in which to generate the image.[10,15] The benefit of using an image-reversal resist is that it has a higher photosensitivity in the image-reversal mode than in the positive mode and its response to irradiation is linear, implying that the topography of the photoresist images the irradiance of the resist directly. In the case of TOP, it is undesirable to use an image reversal or negative resist due to the degradation of the topographical pattern that occurs during the postexposure bake necessary to crosslink the exposed region and reverse the image. The exposed and unexposed regions are effectively scrambled and the intensity pattern generated by the topography on the surface of the resist layer is eroded or lost by diffusion and polymer reflow. To avoid the loss of data in the postexposure bake we used a

positive resist (Shipley STR 1045; $n \sim 1.7$ at $\lambda = 436$ nm) as our imaging medium. When using a positive tone resist, the topography remaining after exposure and development is related to the inverse of the irradiance; the photoresist therefore remains where the irradiance is lowest. While some degradation of the intensity patterns may occur as compared to image reversal resists, we are able to match our theoretical observations to those generated experimentally.

B. Simulations and simple theory

Our numerical calculations of the intensity in the near field of the embossed topography used Fresnel theory.[16,17] Previous theoretical calculations performed in our group to determine the intensity patterns in the near field of an elastomeric photoresist mask used scalar Fraunhofer theory.[18,19] Several groups have shown that scalar theory, while sufficient to describe observations, does not completely describe the system of an elastomeric phase mask or the near-field intensity of light inside a topographically patterned layer of photoresist.[20–22] Rogers and co-workers have described intensity patterns generated through elastomeric masks in thick layers of resist using finite element calculations of the full solutions to Maxwell's equations; the experiment, however, also required careful development of the resist patterns in supercritical CO_2.[23] Ignoring the vector nature of the electromagnetic field generating patterns of intensity will undoubtedly leads to some discrepancies, but the simplicity of Fresnel theory makes it an attractive alternative. We found the results generated here to adequately describe our work.

In modeling our topographically patterned surfaces, we assumed that the surface was illuminated normal to the embossed features by monochromatic, perfectly collimated plane waves, and due to the thickness of the resist, ignored light reflecting back from the silicon substrate. While the light from our source is broadband UV with intensity peaks at 436, 406, and 365 nm, the photoresist is most sensitive to the g line or 436 nm wavelength of light. We used monochromatic, 436 nm light in our calculations for this reason. While the effect of photobleaching that occurs as the layer of resist is exposed is important to lithographic performance,[24] we did not include it in our calculations for simplicity and without causing a noticeable difference between simulation and experiment.

We calculated the intensity pattern resulting from this illuminating field in photoresist layer using Fresnel–Kirchhoff theory[16] and numerically solved a 2D, scalar version of the Fresnel integral [Eq. (1)].

$$E_0(x_o, z_o) = A e^{ikz_o} \sqrt{\frac{ik}{2\pi}} \int e^{ik(x_s - x_o)^2/2z_o} dx_s. \qquad (1)$$

Here E_0 is the electric field at the observation point, z is the distance from the illumination plane to the observation point, and k is the wave number in the photoresist and is equal to $2\pi n/\lambda$, where n is the index of the medium (photoresist, $n = 1.7$) and λ is the wavelength of light. We integrated over the plane of illumination that was taken to be the base of the topographical features on the photoresist ($z = 0$). We chose

the limits of integration to be several times larger than the topographical feature, or for a periodic topography, over a period large enough to prevent edge effects; for most features we integrated over ± 10 μm and calculated the intensity over ± 4 μm. We assumed that the features were infinite along the y axis, and modeled the effect of the topographically patterned surface on the illuminating field as a phase and amplitude perturbation of the illuminating field.

The calculated intensity profiles generated using the surface topography by themselves do not accurately predict the resulting photoresist structures—the process of development can modify the structures. We modeled the development process as isotropic with a dissolution rate linearly proportional both to the optical intensity delivered to the location in the resist and to the surface area of the photoresist exposed to the developing solution.[25] A good photoresist is defined as being at least ten times more likely to dissolve in the developer when exposed than when unexposed.[2] We assumed a selectivity of 100:1 for the photoresist used, confirmed by comparison with experimental structures. We chose an exposure amplitude and performed a single numerical development, stopping at regular intervals to save the curves generated. Because of the linear relationship between exposure and development, we could interchange exposure and development times. Comparison of the height difference between illuminated and unilluminated areas of photoresist at various exposure times enabled calibration of the theoretical and observed structures and confirmed the linear relationship between exposure and development. Figure 2 shows the steps used to generate a theoretical structure.

C. Test patterns and qualitative observations

In evaluating the theoretical approach, we first tested the influence of a phase shift at an isolated step as the simplest theoretical case. We fabricated photoresist masters of rectangular gratings having lines of 10 μm and a periodicity of 20 μm and exposed the embossed surface through an amplitude mask having a dark-field pattern of 50 μm circles. The thickness of the photoresist layer in which the pattern was exposed determined the relative phase at the step edge. The phase step height embossed into the photoresist layer varied with the thickness of the photoresist layer used to generate the master.

Exposure of topographically patterned photoresist through amplitude masks provided simultaneous information about the embossed, and the exposed and developed area. Diffraction occurred at the edges of the metal pattern on the amplitude mask and was also recorded in the photoresist layer.[22] The depth of the relief on the surface of the photoresist and the length of time of the exposure determined the severity of the diffraction. We chose to image areas where both the embossed and exposed resist is visible and the exposed area is largely unaffected by diffraction from the amplitude mask.

We expect rectangular steps embossed on a layer of resist to function similarly to an elastomeric phase-shifting mask. Light passing through the raised portion of the rectangular grating pattern on the surface of a photoresist layer would be
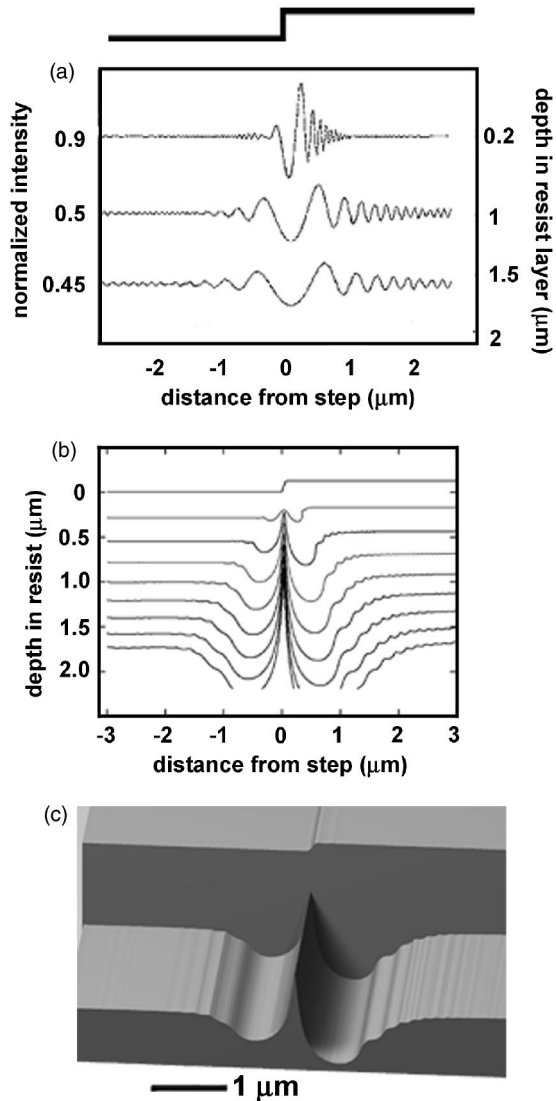
FIG. 2. (a) Plot shows curves at increasing intensity in photoresist arising from an isolated step with a phase depth of π after exposure to flood-UV light. (b) Curves of developed intensity pattern. (c) Theoretical surface generated by plotting the topmost exposure and development curve.

FIG. 3. Comparison of experimental (left) and theoretical (right) surfaces of photoresist embossed with a pattern of 20 μm periodicity having 10 μm lines that serve as isolated edges after exposure and development. The samples were exposed for 7 s through a dark field mask of 50 μm circles. The height of the topography on the mold, and therefore the depth of the embossed features, determined the shift of phase at the step edge.

slowed relative to the light traveling in air in the adjacent recessed portion of the grating. The height of the rectangular step in the photoresist gives the phase difference between the raised and recessed portions of the grating. The features form at the edges of the embossed features. TOP is, in part, an edge lithography, where the edges of the rectangular embossed features become the prominent features in the photoresist pattern: on a thin layer of photoresist, they are the features that remain on the substrate, while on a thick layer of resist, they are the tallest features in the intensity pattern.

D. Factors contributing to the deviation in light intensity from a simple theoretical model

Our first theoretical surfaces differed from our experimental observations in several ways. We initially assumed the rectangular features had perfectly vertical sidewalls and sharp corners. This assumption led to results that were not in
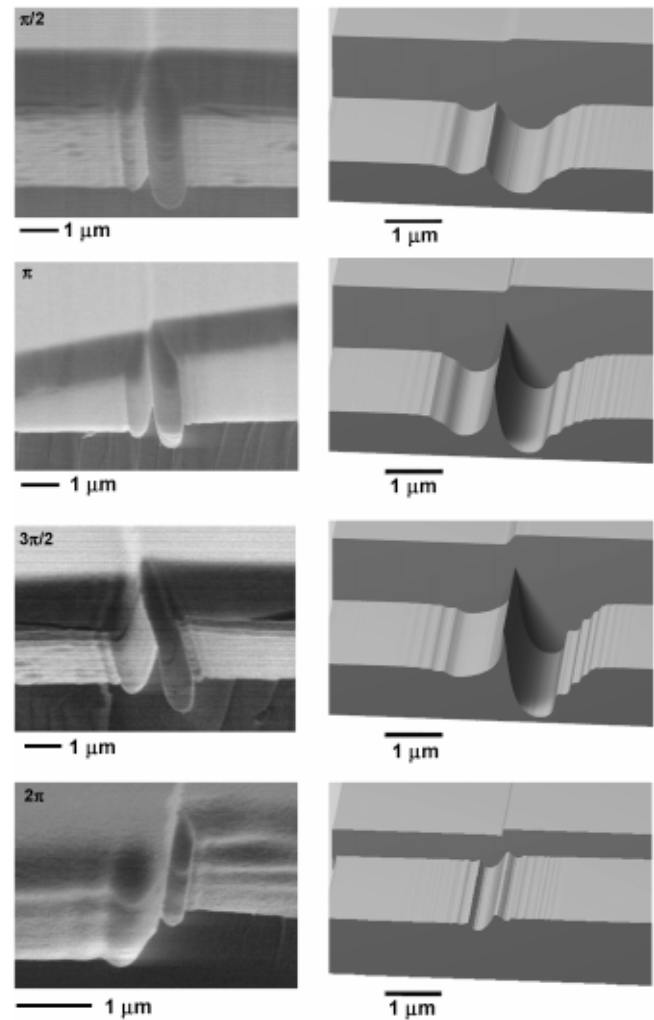
good agreement with our experimental surfaces. We made adjustments to our calculations based on the observation of our embossed surfaces by scanning electron microscopy (SEM). First, we noticed that the sidewalls of our rectangular features were not perpendicular to the photoresist surface. Because of the sidewall profile of the original master was slightly slanted, the light incident on the sidewall was refracted into the step, increasing the intensity under the raised step. Second, because the corners of the embossed features were rounded rather than sharp, we added a lens-like effect at the corners; this effect also increases the intensity of light under the raised step.

Figure 3 shows the theoretical surfaces generated using isolated phase edges modified according to the geometry of the embossed surface observed by scanning electron microscopy. SEM images were obtained with the step going up from left to right. We fabricated the masters at step heights corresponding to phase shifts of $\pi/2$, π, $3\pi/2$, and 2π.

Theoretically, one would expect features arising from a phase shift of π to give the most intense feature, while features arising from phase shifts of $\pi/2$ and $3\pi/2$ to be somewhat less intense, and phase shifts of 2π to give no features.

In the case of the first three step heights, the surfaces obtained theoretically and experimentally agree both with expectations and with each other, including the sharpness of the peak of intensity and the relative depths of the trenches on either side of the peak. We did not observe experimentally as many ripples arising from diffraction as are predicted by the theory. This difference was expected since the light source used in the simulation was monochromatic (436 nm), whereas the experimental light source had three significant spectral peaks (436, 406, and 365 nm). The interference arising from the three wavelengths caused the diffraction ripples to blur. In the case of the 2π phase shift, however, the difference between our expectation and experimental result was more pronounced. When using a broadband UV light source, the height of the step will never be simultaneously out of phase for all three spectral peaks. Instead, the wavelengths for which the step height was not 2π contributed to make a small intensity peak at the edge of the embossed feature. We modeled this effect for the 2π step as a short exposure of a phase difference of 2.4π, corresponding to a low exposure dose at 365 nm; this theoretical structure agreed well with the experimental image.

E. Imaging the intensity profiles of rectangular gratings with higher periodicities

After becoming confident that our theoretical framework adequately described and predicted our experimental results at isolated rectangular phase steps, we considered gratings having higher periodicities: 4 μm periodicity having lines of 2 μm and 2 μm periodicity having lines of 1 μm. The depth of the features was selected to be equal to a π phase shift (300 nm). In these rectangular gratings, the phase edges were close enough together that interference became important. We examined the embossed samples by SEM to determine the average tilt of the sidewall and modified our theoretical grating accordingly. Comparisons of theoretical and experimental results for rectangular gratings are shown in Fig. 4. Both rectangular gratings had the most intense features at the recessed edges of the embossed step and the deepest trenches under the raised step as a result of the slanted sidewall and curved corner. Both qualities were predicted in the experiments and simulations of a single edge with a step height equal to π. Theoretically simulated and experimentally observed surfaces match well for both periodicities.

We also tested a rectangular grating that we fabricated using soft lithography. The raised features are 190 nm tall, 130 nm wide, separated by 700 nm, and embossed on a thick layer of photoresist (Fig. 5). Because the embossed features are close to a phase shift of $\pi/2$, the most intense peaks arise under the recessed portion of the grating when exposed. This result is predicted both by the isolated edge with a step height equal to a phase shift of $\pi/2$ and by the theoretical
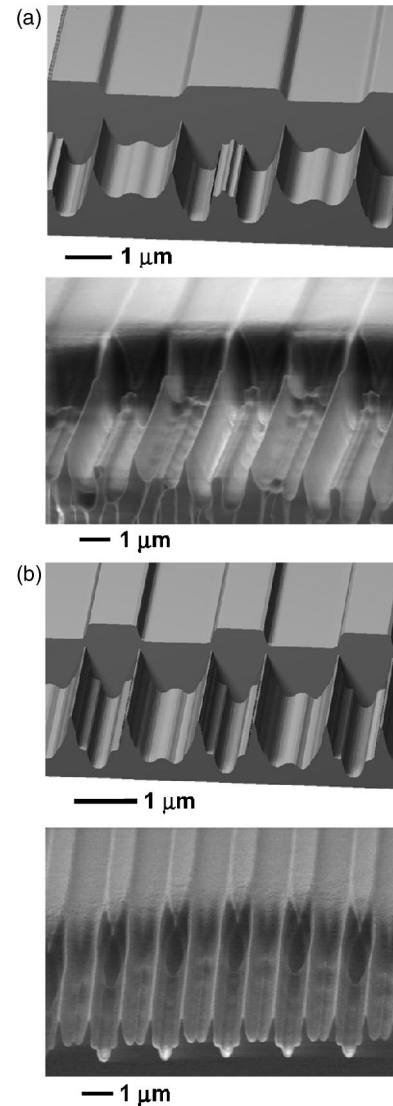

(a)

— 1 μm

— 1 μm

(b)

— 1 μm

— 1 μm

FIG. 4. Comparisons of experimental and theoretical embossed, exposed, and developed rectangular gratings at a phase depth of π. Images in (a) show embossed and exposed surfaces with a period of 4 μm (2 μm lines) and a depth of 300 nm and exposure time of 7 s. Images in (b) show surfaces with a period of 2 μm (1 μm lines) having a depth of 300 nm and an exposure time of 5 s.

simulation for a grating with these features. The intensities of the peaks are not as high in the predicted structure as in the experimentally observed structure, but the theory accurately predicts the equally spaced features with larger depths arising under the recessed region than under the raised region of the grating.

F. Imaging the intensity profiles for convex lens-like structures

Geometrical optics predicts that plane waves impinging on a transparent, dielectric, spherical surface will be reshaped into spherical waves and will converge to a focal point. We generated an array of convex lenses using soft lithography,[11] molded the lenses in PDMS, and embossed them on a layer of photoresist. The photoresist lenses were
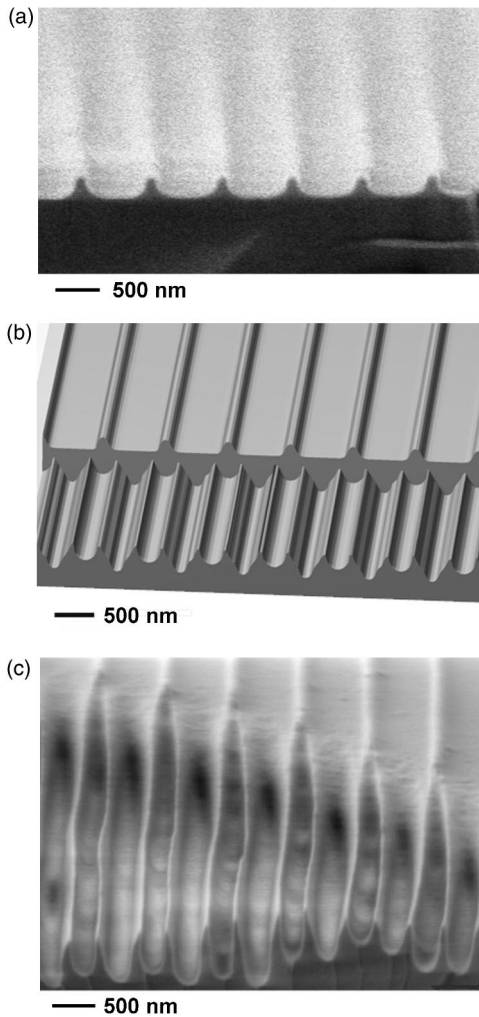
FIG. 5. Grating pattern generated by soft lithography embossed and exposed on a thick layer of photoresist. Features 190 nm tall and 130 nm wide embossed in the resist layer are shown in (a). Image (b) shows the embossed and exposed theoretical surfaces for the grating. The exposed surface corresponds well with (c), a SEM image showing a surface embossed and exposed through an amplitude mask for 3 s.

then exposed, developed, examined by SEM, and compared with theoretical simulation. The exposed and developed photoresist pattern shows the path of the diffracting light under the lens rather than a single focal point. Figure 6 shows a line plot of the simulated structures as the exposure intensity increases at the top. Images obtained by SEM of the embossed and exposed surfaces match well with the predictions.

G. Imaging the intensity profiles for smoothly changing surfaces

Holographic diffraction gratings, produced by interference of two laser beams, provide a sinusoidal surface topography and are commercially available at several wavelengths. We showed previously that the features generated by an exposure of sinusoidal topography embossed on a layer of photoresist arose under the concave portion of the grating.[4] We theorized that the surface embossed with a sinusoidal pattern acted as an array of convex and concave lenses, where the
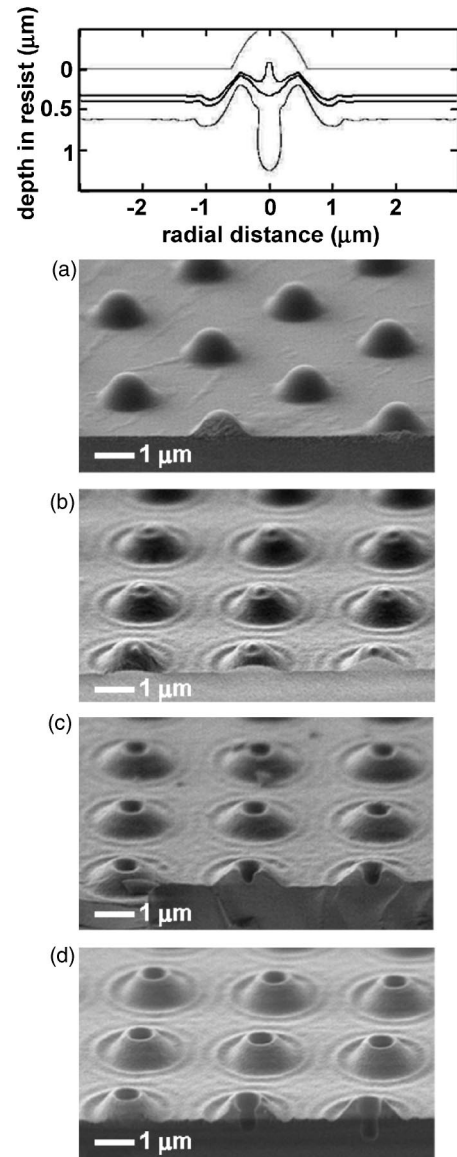

FIG. 6. Comparison of theoretical line plots and experimental images for 1.5 μm lenses; line plot showing the predicted pattern after exposure and development is shown at the top: (a) SEM of a layer of photoresist embossed with 1.5 μm lenses, (b) 3.5 s exposure of embossed lenses, (c) 4 s exposure, and (d) exposure of 4.5 s.

convex portion of the grating focused the light into the photoresist layer under the convex feature, and the concave portion of the grating dispersed the light into the layer, thereby protecting the features directly underneath.

Figure 7 compares theoretical profiles for a sinusoidal grating with a period of 417 nm at several exposure intensities with SEM images of a surface embossed with the grating and exposed for 8, 11, and 14 s. The theoretical profile shows the topography of the smoothly changing embossed surface in the rear, with exposed surfaces at increasing intensities in the front. The first simulated pattern generated using the embossed surface agrees well with both the experimental observation for a thin layer of resist and for a short exposure time on a thick layer of resist [Figs. 1 and 5(a), respectively].
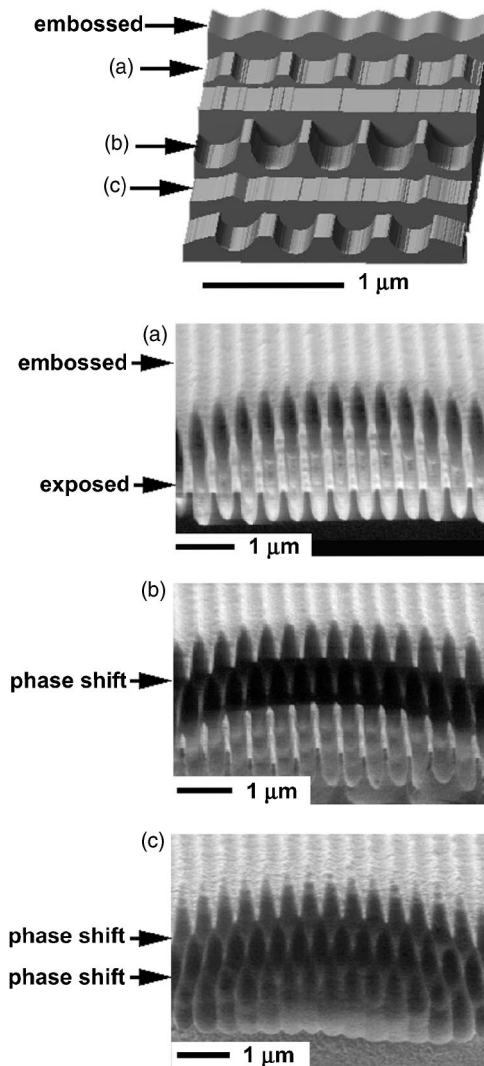
FIG. 7. Comparison of theoretical and experimental surfaces embossed and exposed with a sinusoidal grating having a period of 417 nm. The image at the top shows the theoretically simulated embossed and exposed surfaces at several exposure intensities. The theoretical levels are labeled to correspond with the SEM images: (a) surface exposed through a mask of 5 μm circles for 8 s with the features arising under the concave portion of the grating; (b) surface exposed for 11 s and showing the features appearing under the convex portion of the grating; and (c) exposure of 14 s and a null in intensity, where the features are pinched off in the center of the circle. The wall of the exposed circle traces the history of the intensity pattern.

Further, the theoretical profile predicted that features arising from a sinusoidal grating embossed on thick layers of resist and exposed to UV light would pass through a null, where no features would be observed, to a region where the features would reappear under the convex portion of the grating, as shown in (b). The null and shift in the location of the features occurred due to the interference generated by the periodicity of the embossed surface; a SEM image of the second null is shown [Fig. 7(c)].

IV. CONCLUSIONS

Topographically directed photolithography is a simple, parallel technique for generating nanostructures. Large areas can be embossed and exposed; neither a stepper nor elaborate optics is required. By tuning the depth of the topography embossed on the resist layer, TOP can operate at a variety of wavelengths. TOP can also be used to generate nanostructures on curved surfaces[8,9] and for use with other techniques.[8,22,26] The disadvantages of the technique are that it is difficult to register the embossed pattern through the layer of photoresist to underlying features, that the use of an elastomeric stamp limits the dimensional stability of the embossed features, and that the embossed pattern of photoresist may deviate somewhat from the pattern on the stamp. Placing the elastomeric mold on a rigid backing or using a more rigid polymer would increase the dimensional stability and could allow through-mask alignment for pattern registration with thin layers of photoresist.[27,28] Using more rigid polymers or backings could compromise the ability to pattern curved surfaces.

Photoresist structures generated by TOP can be predicted from the structure of the embossed topography using the Fresnel diffraction theory; the theoretical surfaces agree well with structures obtained experimentally. A limitation of our theoretical technique is the difficulty of solving the inverse of the Fresnel integral and reversing the process of development—we cannot easily determine the topography necessary to fabricate a specific pattern. An alternative approach is to design a topographical surface and test it by simulating exposure and development. Using only the scalar nature of light is also a limitation in the theoretical results; future experiments could use rigorous solutions of Maxwell's equations to more completely describe the patterns of light intensity generated. Rigorous theoretical treatment may also permit calculation of embossed features necessary to produce a desired resist pattern.

[1]M. Madou, *Fundamentals of Microfabrication* (CRC, Boca Raton, Fla., 1997).
[2]W. M. Moreau, *Semiconductor Lithography: Principals and Materials* (Plenum, New York, 1988).
[3]P. Rai-Choudhury, in *Handbook of Microlithography, Micromachining, and Microfabrication*, edited by A. J. Moses and J. Wood (SPIE Optical Engineering Press, Bellingham, WA, 1997), Vol. 1, p. 768.
[4]K. E. Paul, T. L. Breen, J. Aizenberg, and G. M. Whitesides, Appl. Phys. Lett. **73**, 2893 (1998).
[5]Y. Xia and G. M. Whitesides, Angew. Chem., Int. Ed. Engl. **37**, 550 (1998).
[6]Y. Xia, J. A. Rogers, K. E. Paul, and G. M. Whitesides, Chem. Rev. (Washington, D.C.) **99**, 1823 (1999).
[7]E. Kim, X.-M. Zhao, and G. M. Whitesides, Adv. Mater. (Weinheim,

Ger.) **9**, 651 (1997).

[8]A. J. Black, K. E. Paul, J. Aizenberg, and G. M. Whitesides, J. Am. Chem. Soc. **121**, 8356 (1999).

[9]K. E. Paul, M. Prentiss, and G. M. Whitesides, Adv. Funct. Mater. **13**, 259 (2003).

[10]J. Aizenberg, J. A. Rogers, K. E. Paul, and G. M. Whitesides, Appl. Opt. **37**, 2145 (1998).

[11]C. Marzolin, St. P. Smith, M. Prentiss, and G. M. Whitesides, Adv. Mater. (Weinheim, Ger.) **10**, 571 (1998).

[12]www.advancedrepro.com

[13]www.photronics.com

[14]S. Jeon, E. Menard, J.-U. Park, J. Maria, M. Meitl, J. Zaumseil, and J. A. Rogers, Adv. Mater. (Weinheim, Ger.) **16**, 1369 (2004).

[15]J. Aizenberg, J. A. Rogers, K. E. Paul, and G. M. Whitesides, Appl. Phys. Lett. **71**, 3773 (1997).

[16]S. G. Lipson, H. Lipson, and D. S. Tannhauser, *Optical Physics* (Cambridge University Press, Cambridge, 1995).

[17]M. Born and E. Wolf, *Principals of Optics* (Pergamon, New York, 1993).

[18]J. A. Rogers, K. E. Paul, R. J. Jackman, and G. M. Whitesides, Appl.

[19]Phys. Lett. **70**, 2658 (1997).

[19]J. A. Rogers, K. E. Paul, R. J. Jackman, and G. M. Whitesides, J. Vac. Sci. Technol. B **16**, 59 (1998).

[20]Z.-Y. Li, Y. Yin, and Y. Xia, Appl. Phys. Lett. **78**, 2431 (2001).

[21]J. Maria, S. Jeon, and J. A. Rogers, J. Photochem. Photobiol., A **166**, 149 (2004).

[22]M. Paulus, B. Michel, and O. J. F. Martin, J. Vac. Sci. Technol. B **17**, 3314 (1999).

[23]S. Jeon, J.-U. Park, R. Cirelli, S. Yang, C. E. Heitzman, P. V. Braun, P. J. A. Kenis, and J. A. Rogers, Proc. Natl. Acad. Sci. U.S.A. **101**, 12428 (2004).

[24]R. Dammel, *Diazonapthoquinone-based Resists* (SPIE Optical Engineering Press, Bellingham, WA, 1993).

[25]Y. Cheng, C.-Y. Lin, D.-H. Wei, B. Loechel, and G. Gruetzner, J. Microelectromech. Syst. **8**, 18 (1999).

[26]J. C. Love, K. E. Paul, and G. M. Whitesides, Adv. Mater. (Weinheim, Ger.) **13**, 604 (2001).

[27]T. Burgin, V.-E. Choong, and G. Maracas, Langmuir **16**, 5371 (2000).

[28]J. G. Goodberlet, Appl. Phys. Lett. **76**, 667 (2000).